Applied Energy 403 (2026) 127069

Contents lists available at ScienceDirect

Applied Energy

journal homepage: www.elsevier.com/locate/apen

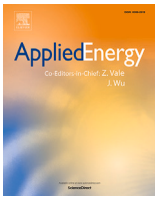

Can distributed hydrogen production improve the earthquake resilience of power systems?

Melissa Alé [a,*], Madhura Yeligeti [b], Rafaella Canessa [c], Manuel Wetzel [b], Rodrigo Moreno [a], Rebecca Peer [c], Hans-Christian Gils [b], Jannik Haas [c]

[a] Department of Electrical Engineering, University of Chile, Tupper 2007 Avenue, Santiago, 8370451, Metropolitan Region, Chile
[b] German Aerospace Center (DLR), Institute of Networked Energy Systems, Curiestr. 4, Stuttgart, 70563, Germany
[c] Department of Civil and Natural Resources Engineering, University of Canterbury, 69 Creyke Road, Christchurch, 8041, Canterbury, New Zealand

HIGHLIGHTS

- Analysis of diverse spatial hydrogen distributions for grid resilience.
- Hazard modeling integrated into power system resilience assessment.
- Distributed hydrogen demand demonstrates superior resilience in seismic scenarios.

GRAPHICAL ABSTRACT

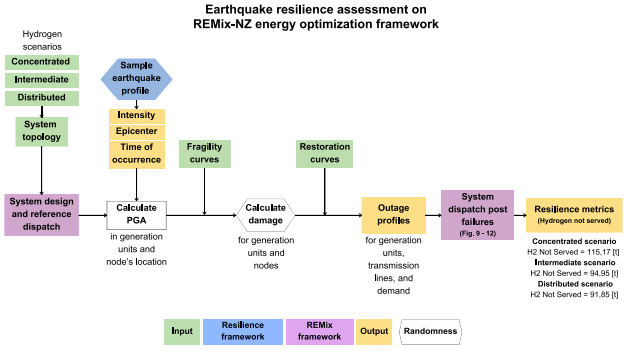

ARTICLE INFO

Keywords:
Energy system modeling
Resilience planning
Model coupling
Earthquake modeling
Hydrogen integration

ABSTRACT

Resilience planning is crucial for sustainable energy transitions, particularly in mitigating the impacts of extreme weather events and natural hazards. This study examines the integration of hydrogen as a new energy carrier, focusing on its technical flexibility and potential stresses. We connect a resilience framework comprising four phases—hazard characterization, system component vulnerability assessment, power system response, and recovery—to an energy system optimization model. This tool plans the capacity expansion with economic dispatch under contingency scenarios to calculate resilience metrics, including energy not served and generation availability. To demonstrate the methodology, a case study on New Zealand compares the effects of three hydrogen spatial distribution scenarios: concentrated, intermediate, and distributed. Results indicate that a distributed hydrogen scenario enhances resilience by reducing unserved electricity and unmet hydrogen demand while achieving the lowest total system costs. These findings support adopting a nationwide distributed hydrogen hub strategy to improve system adaptability. The proposed framework is scalable and adaptable to other countries, providing a robust tool for integrating resilience into energy planning.

* Corresponding Author.
Email address: melissa.ale@ug.uchile.cl (M. Alé).

https://doi.org/10.1016/j.apenergy.2025.127069
Received 21 January 2025; Received in revised form 14 October 2025; Accepted 9 November 2025
Available online 18 November 2025

1. Introduction

1.1. Context and motivation

The energy transition represents an urgent global challenge, driven by the need to mitigate climate change, enhance energy security, and meet the growing demand for clean and sustainable energy. Transitioning to a low-carbon economy hinges on leveraging renewable resources and integrating emerging energy carriers, such as hydrogen [1]. However, achieving these goals requires resilient planning for national electricity systems to address technical challenges, including supply intermittency and complex demand management.

Reliable and resilient planning are complementary pillars in the energy transition, addressing routine disturbances and rare catastrophic events, respectively. Reliability ensures consistent system operations under expected conditions [2], while resilience prepares systems to withstand and recover from high-impact disruptions [3]. This dual approach is indispensable for modern energy systems, which are becoming increasingly complex due to integrating renewable energy sources, advanced technologies, and diverse sectors such as heat, transportation, and industry [4]. As natural disasters and extreme weather events continue to grow in frequency and intensity [5], advanced planning tools are critical to balancing reliability and resilience [6], safeguarding infrastructure integrity while enabling rapid recovery from disruptions [7].

Managing the energy transition effectively requires advanced planning tools to optimize energy systems by balancing multiple objectives [8] and multiple services [9]. These tools address the inherent complexity of modern systems through methodologies such as linear and nonlinear programming, probabilistic approaches, and graphical techniques. Python-based solvers, for instance, provide robust frameworks for optimizing single- and multi-objective problems, offering capabilities for linear, quadratic, and mixed-integer programming [10]. Notable examples include PyPSA [11,12], which supports power flow optimization and security-constrained analyses, and FINE [13], which enables integrated assessments across multiple energy sectors. However, while important for system optimization, these tools lack integrated capabilities for contingency analysis and resilience metrics—key aspects for addressing the challenges posed by high-impact disruptions.

The REMix (Renewable Energy Mix) framework [14], developed by the German Aerospace Center (DLR), addresses these gaps. For context, this linear optimization tool for system expansion and operation is based on GAMS, and uses commercial solvers such as CPLEX [15] and GUROBI [16]. Designed to facilitate the integration of renewable energy sources [17] and hydrogen technologies [18], REMix identifies the lowest-cost investments and multi-sectoral operations across electricity, transport, and heat systems. Through the integration of resilience metrics and contingency analysis, as proposed in this study, REMix has the potential to address the challenges posed by high-impact, low-probability (HILP) events, thereby becoming a key tool for advancing resilient energy systems.

In the context of energy systems, resilience is defined as the capacity of a grid to anticipate, withstand, recover, and adapt its infrastructure and operations to HILP events [19]. A resilient energy system must fulfill several essential functions: it must anticipate potential crises, prepare by defining actionable measures to mitigate system degradation, adapt operations to respond effectively, recover swiftly to restore power supply and infrastructure, and maintain critical operations to ensure the continued functionality of essential services [3]. These capabilities underscore the need for resilience planning and evaluation frameworks to enhance system adaptability and ensure long-term reliability.

The resilience curve, illustrated in Fig. 1, represents the typical response of an energy system to a disruptive event. This curve often assumes that the system returns to its initial state after the event [20]. However, alternative behaviors, such as adaptive resilience, depict systems reorganizing to surpass their initial conditions after compensating for losses [21]. Conversely, non-resilient behaviors, such as ductile or collapsing responses, reflect systems that either stabilize at reduced functionality or fail entirely to recover [22]. These dynamics highlight the importance of quantitative assessments in understanding system performance under stress and in informing the development of targeted resilience strategies.

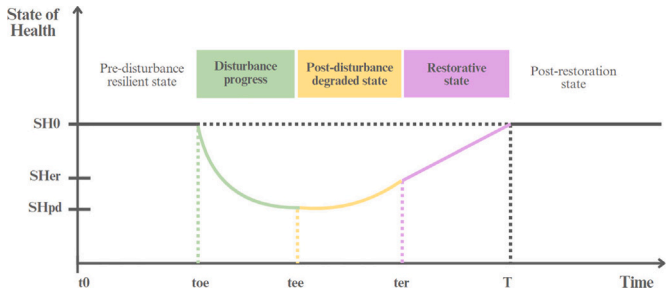

Fig. 1. Graphic representation of a resilience curve over time. Own elaboration based on [23].

The behavior of the resilience curve [23] varies significantly across systems, allowing the quantification of a system's *health state* through resilience indicators. These indicators are integral to cost-benefit analyses for resilience planning, as shown in [24]. Due to the absence of a universally expected system behavior under disruptive events, multiple metrics have been developed to evaluate both operational and infrastructure resilience. Operational metrics assess the effectiveness of post-event restoration measures [25], while infrastructure metrics evaluate the seismic vulnerability of critical power system components, such as generators, transmission lines, and substations. Additionally, they consider cascading failures caused by infrastructure interdependencies, quantifying the impact of catastrophic events [26]. These metrics are essential for identifying vulnerabilities and guiding the design of resilient energy systems.

Given the destructive potential of events affecting energy systems, resilience planning is indispensable. Numerous studies have developed structured methodologies for resilience planning and assessment. For instance, the framework proposed in [27] emphasizes a four-phase approach, which includes hazard profiling, correlating hazard intensity with damage probabilities through fragility curves, and defining system response and recovery functions. Spatiotemporal hazard simulations and iterative processes complement these stages to validate the sequence of information required for resilience metrics. Furthermore, critical outputs for resilience assessments, identified in [28–30], underscore the importance of comprehensive frameworks to evaluate and enhance energy system resilience.

Such methodologies have been successfully applied to power system expansion planning [31]. These applications illustrate how structured resilience assessments inform the development of robust energy infrastructures capable of withstanding and recovering from high-impact disruptions.

Resilience planning addresses a wide range of hazards, including natural disasters such as earthquakes, as demonstrated in studies on network planning [7], decision-making algorithms [31], cascading damage analyses [32], and simulation-based optimizations to enhance seismic resilience [33]. Damage assessments of electrical substations [34] provide further insights into vulnerability. Other studies explore the impacts of volcanic activity [35] and extreme weather conditions, such as typhoons [36] and wind variability [37], emphasizing strategies like proactive generation dispatch to minimize load loss. Notably, the resilience assessment methodologies discussed in the literature are sufficiently flexible to be parameterized for various event types, demonstrating their adaptability to different contexts and challenges.

The resilience of an electrical network, or its *state of health*, is quantified through resilience metrics, which systematically evaluate system performance under disruptive events. These metrics can be categorized as performance-based or non-performance-based [24]. Performance-based metrics, such as energy not served (the total undelivered electrical energy) [33] and unsupplied load (the unmet instantaneous power demand) [38,39], are derived directly from system behavior simulations like Monte Carlo methods. In contrast, non-performance-based metrics, informed by site visits and damage statistics, evaluate factors influencing system performance before, during, and after an event. Together, these metrics offer complementary insights into operational and infrastructural resilience.

A prominent resilience metric for earthquake assessments is the *FLEP metric* [40], which has been applied in studies such as [7,33]. This metric evaluates four critical aspects: the rate of resilience decline (Φ) and the severity of the decline (Λ) during the disturbance phase, the extent (E) of the post-disturbance degraded phase, and the speed (Π) of recovery to the pre-event state. By quantifying how quickly resilience drops, the impact's severity, the damage's scope, and the recovery efficiency, FLEP provides a comprehensive framework for assessing system health during and after HILP events. This metric is particularly relevant for designing strategies to enhance resilience in systems exposed to seismic risks.

As previously discussed, resilient energy system planning has focused on expanding generation and transmission capacities. Hydrogen integration is promising because of its decarbonization potential across sectors [42] and because it can enhance system security [41] and flexibility [43,44]. Studies such as [45,46] have analyzed the resilience benefits of integrating hydrogen into energy hubs and its impact on operational performance. Additionally, research highlights improvements in distribution network resilience through hydrogen systems [47]. These findings underscore the role of hydrogen as a critical element in building adaptive and resilient energy systems.

In the context of the global energy transition and diversification of electricity systems, hydrogen is increasingly recognized as a promising energy vector. Studies in New Zealand [48,49], Australia [50], the European Union [51], and Colombia [52] emphasize its flexibility as essential for achieving decarbonization and carbon neutrality targets. Large-scale hydrogen integration requires meticulous planning that addresses factors such as the production of pink hydrogen [53] or gray hydrogen [54], storage availability in hybrid systems [55,56], and the optimization of hydrogen integration into energy systems [57]. This planning must not only consider investment and operational costs but also account for externalities, including carbon emissions and environmental impacts, to ensure sustainable and resilient energy transitions.

Building on this research gap, this study examines the critical role of hydrogen in enhancing grid resilience within renewable energy-dominated systems. While integrating renewable energy sources such as hydro, wind, and solar is essential for decarbonization, it introduces vulnerabilities due to their variability and location-specific constraints. Coupled with the increasing frequency of natural hazards—such as earthquakes, extreme weather events, and climate-induced disruptions—these factors demand innovative strategies to ensure a reliable electricity supply and system adaptability. Despite global efforts to integrate hydrogen as a versatile energy carrier, the technical and strategic challenges of balancing sustainability with resilience remain underexplored.

To address this gap, this study employs a structured four-phase resilience framework that includes hazard characterization, system component vulnerability assessment, power system response, and recovery analysis. This framework is integrated into a robust energy system optimization tool, capable of modeling system expansions, economic dispatch, and contingency scenarios. By simulating different hydrogen production topologies—distributed, intermediate, and concentrated—under various hazard conditions, the methodology offers a comprehensive approach to evaluating resilience metrics such as energy not served and generation availability.

1.2. Contribution and research questions

This study presents a novel contribution by integrating a four-phase resilience framework with the national-scale REMix energy system optimization model. It offers, for the first time, an explicit evaluation of the role of hydrogen in enhancing the seismic resilience of a real power system. Specifically, it compares large-scale centralized and small-scale distributed hydrogen demand layouts using the REMix energy system modeling framework. This dual contribution—methodological innovation and applied analysis—shows that the spatial configuration of hydrogen demand (centralized vs. distributed) can fundamentally alter resilience outcomes on a national scale. This structured approach provides actionable insights to improve grid resilience and is scalable and adaptable to other countries.

The following research questions guide this study:

- How can a resilience framework be integrated with an energy optimization framework, such as REMix, to evaluate the role of hydrogen in enhancing power system resilience?
- Considering future uncertainties and disruptions, how can power system resilience be effectively assessed during energy transitions?
- How do different spatial distributions of hydrogen resources, such as distributed small-scale versus concentrated large-scale configurations, impact system resilience, and adaptability?

Answering the above questions is important for three reasons:

1. The shift toward renewable electricity-dominated systems worldwide necessitates resilient planning, which can be achieved through advanced optimization frameworks like REMix.
2. The increasing frequency and intensity of severe weather events and natural disasters further emphasize the need for proactive measures to ensure power systems can withstand, recover from, and adapt to disruptions.
3. Hydrogen's role as an energy vector can enhance system flexibility. However, integrating hydrogen into energy systems presents significant technical challenges, requiring a carefully designed and strategically implemented approach to ensure both reliability and resilience across diverse energy contexts.

Overall, this research contributes to the broader understanding of resilient power system planning related to integrating hydrogen and offers insights transferable to other countries.

1.3. Outline

The remainder of this paper is organized as follows: Section 2 outlines the methodology, detailing how the resilience assessment is connected to the REMix framework and describing the defined scenarios. Section 3 presents and discusses the results obtained from the model applications. Finally, Section 4 summarizes the key conclusions and suggests directions for future research.

2. Methods and model description

This section details the framework employed to analyze the resilience of a national power system using the REMix energy optimization framework. The information flow from the resilience framework to the REMix model is first outlined. Subsequently, the phases constituting the resilience framework and the configuration of the optimization model are described in detail. Finally, the hydrogen demand scenarios used to construct the case studies are presented.

Fig. 2 illustrates the proposed modeling approach, highlighting the model inputs, outputs, and key processes. The inputs include the system topology for each hydrogen scenario and the parameters defining a natural disaster, represented by electrical components' fragility and restoration curves. Additionally, stochastic processes are incorporated to simulate the occurrence of a natural disaster and the system's pre-event

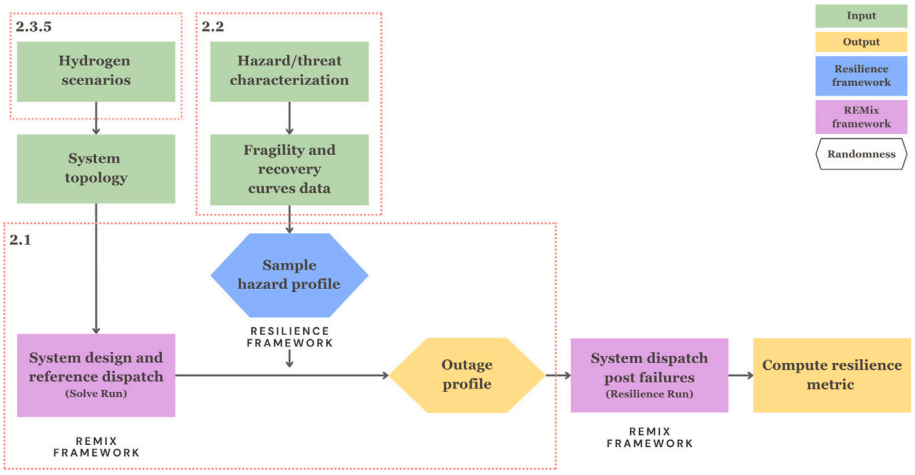

Fig. 2. General modeling approach. The numbers below refer to the subsections where more information is provided. 2.1 shows the connection between the resilience and REMix frameworks. 2.2 details resilience modeling. 2.3.5 defines hydrogen demand scenarios.

operation. The model outputs comprise system disconnection profiles, post-disaster operational performance, and resilience metrics obtained through REMix optimizations.

2.1. Modeling approach

This research employs a three-stage procedure—*Fragility Modeling*, *Failure Simulations*, and *Resilience Metrics*—integrated within a four-phase resilience assessment framework, as depicted in Fig. 3.

The first stage, *Fragility Modeling*, establishes the system's topology and operational state under normal conditions prior to any disturbances. In this stage, data is collected to characterize natural hazards and to model potential damage to electrical system components, along with their subsequent restoration. This is achieved through the use of fragility and restoration curves, which quantify the vulnerability and recovery dynamics of system elements.

The second stage, *Failure Simulations*, involves the random selection of parameters defining a natural hazard to estimate the probability of damage to each power system component. Based on these probabilities, capacity reductions and disconnection profiles are determined, which, in turn, influence the system's operational performance following faults. These disconnection profiles enable an evaluation of the system's response regarding infrastructure and capacity losses impacting the ability to meet demand.

The final stage focuses on calculating *Resilience Metrics*, following rigorous testing. These metrics quantify the average energy not supplied due to disconnections triggered by natural hazards, providing a robust measure of the system's resilience.

2.1.1. REMix energy optimization framework

The optimization framework employed in this study is REMix [14], a comprehensive and flexible tool for modeling multi-energy systems with high spatial and temporal resolution.

REMix adopts a multi-nodal approach, where nodes are interconnected through various energy carrier networks. Within each region, all units of a specific technology are aggregated and treated as a single entity.

The framework enables the analysis of system capacity expansion and hourly operation over the entire time horizon, optimizing these aspects comprehensively in a single run. REMix minimizes the aggregated investment and operational costs for expanding generation, transmission lines, and storage capacity, considering system requirements and renewable resource potential.

The resilience methodology incorporated into REMix allows for integrating outage profiles for generation technologies and transmission lines, as well as demand changes [59]. This methodology modifies the optimization process, which is conducted in two consecutive stages [60]:

Solve Run: In this stage, system expansion is optimized to determine the installed capacities for each technology for a selected year. This process considers resource availability and minimizes both investment and operational costs, constructing the system and establishing a baseline scenario to analyze its performance under normal conditions.

Resilience Run: This stage focuses solely on operational optimization without expanding the system. It incorporates disconnection profiles through an additional parameter, representing functionality as a time series. The system's operation is then analyzed to evaluate its response to the disconnection of generation, transmission, and demand caused by an extreme and unforeseen event.

Resilience metrics can be calculated by contrasting the baseline operation from the *Solve Run* with the disrupted operation in the *Resilience Run*. These metrics assess infrastructure resilience and quantify energy demand not served due to contingencies associated with extreme events.

2.2. Resilience assessment

The resilience assessment conducted in this study comprises four main phases, as originally presented in [27]:

1. Hazard characterization: Historical data are analyzed to generate thousands of scenarios, each describing a natural disaster's intensity and spatiotemporal characteristics. This phase provides detailed information on the occurrence and impact of potential disruptive events.

2. System component vulnerability evaluation: Fragility curves are employed to estimate the probability of disconnection for each electrical system component under a given disaster intensity. This information is then used randomly to determine the percentage of disconnections across the network.

3. Electrical system response: This phase evaluates the reorganization of the system's operation after the disconnection of generation and transmission units caused by a natural disaster. It examines how available electrical units in the network are utilized to meet demand under disrupted conditions.

4. Electric system recovery: The optimization process integrates restoration efforts for both infrastructure and operations. Restoration curves are used to estimate the recovery time required for each technology to fully restore its operational capacity to 100 %.

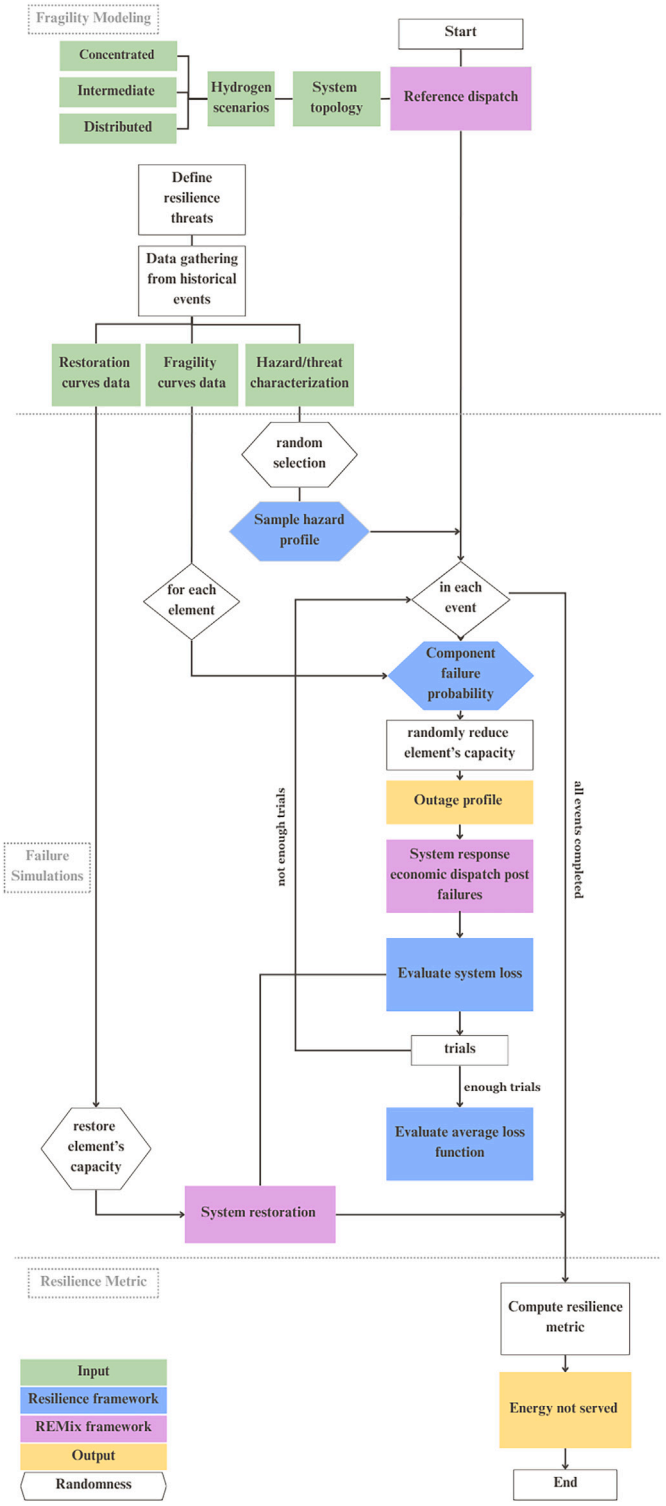

Fig. 3. Detailed methodology flowchart. Own elaboration based on [3,28–30,58] visualizations.

2.2.1. Earthquake characterization

Earthquakes are HILP events that pose significant risks to electrical systems. Due to their inherently unpredictable nature, these events are associated with considerable uncertainty. The extent of damage to each system component is determined probabilistically using fragility curves.

An earthquake, characterized by a defined epicenter (latitude and longitude), intensity, and depth, can be analyzed to assess its impact on the electrical system. This is achieved by calculating the Peak Ground Acceleration (PGA) at each location where electrical components are situated. The PGA quantifies the level of ground shaking caused by the earthquake, serving as a key parameter to characterize the event. By associating the PGA with fragility curves, it is possible to estimate the probability of damage to electrical components and assign an intensity measure to the natural hazard.

The PGA [61], measured in gals, is calculated using the Eq. (1):

$$PGA(r,h,M) = \frac{e^{-2{,}73\ log(r+1.58\ exp(0.608\cdot M))} \cdot e^{6.36+1.76\cdot M+0.00916\cdot h}}{980.665} \quad (1)$$

where M is the magnitude intensity of the earthquake on the Richter scale, h is the depth of the earthquake determined by the hypocenter (ex, ey, h), and r is the radius that determines the distance between the epicenter (ex, ey) and the location (x, y) of a given electrical component, calculated according to the Eq. (2):

$$r = \sqrt{(ex-x)^2 + (ey-y)^2} \quad (2)$$

2.2.2. Vulnerability assessment

Assessing the vulnerability of electrical system components to HILP events is essential for understanding the extent of potential structural damage. Earthquakes, due to their instantaneous and disruptive nature, can cause significant disturbances within the system.

Fragility curves enable the prediction of the potential damage state of an electrical component based on specific event parameters and geographical location. The PGA is calculated for each electrical component in its specific position according to the earthquake's defined intensity and hypocenter. This calculation allows for determining the probability associated with each damage state (complete, extensive, moderate, and slight) by comparing the likelihood of a given damage state to another previously graphically defined state.

Fragility curves can be derived from empirical data through statistical analysis of observed years, analytical determination based on a specific simulation model, or experimental determination through deliberate component failure. Fig. 4a presents the fragility curves of generation units and high-voltage electrical substations used in this study. The curves are based on information from the HAZUS Earthquake Modeling Manual [62], which describes the behavior of the units according to lognormal distribution functions. These functions provide the probability of reaching or exceeding different damage states given a specific PGA.

2.2.3. Restoration data

The restoration of an electrical component's total capacity is governed by recovery curves, which depict the time required to regain full functionality following earthquake-induced damage. These curves are modeled using a normal distribution function, based on HAZUS Earthquake Modeling Manual data, as illustrated in Fig. 4b. The recovery curves provide a probabilistic representation of the restoration process, capturing variations in recovery times across different components and damage levels.

The HAZUS manual for earthquake modeling, although based on U.S. data, is justified for use in modeling damage to New Zealand's electrical system due to its robust methodology, which incorporates multiple variables and scenarios, making it adaptable to other contexts. Additionally, as most New Zealand studies focus on buildings and cables, the lack of local data specific to electrical components supports its application. Lastly, the universal principles of earthquake engineering, with minimal regional variations, further validate the global applicability of HAZUS-based insights.

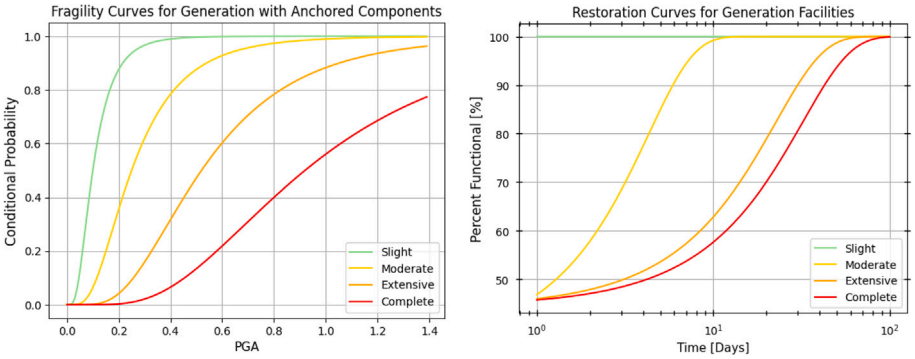

(a) Fragility curve for generation units. (b) Restoration curve for generation units.

Fig. 4. Fragility curves for power system components Own elaboration based on HAZUS Earthquake Modeling Manual data [62].

2.2.4. Resilience metrics

To evaluate the electricity system's resilience in the context of hydrogen production, specific metrics have been selected based on outcomes from optimizing system operations in REMix. The *FLEP metric* [40] measures infrastructure and demand resilience by analyzing the temporal behavior of connected generation and demand curves. Additionally, energy not served is quantified as the difference between demand and generation output, derived directly from REMix optimizations. A more resilient system exhibits minimal energy not served during HILP events.

For earthquake scenarios, the resilience metrics L, E, and P are employed to assess system performance over time. These metrics address critical resilience aspects:

- L (Low): This metric answers the question, "How *low* is the state of health of the system?" It represents the percentage reduction between the pre-event capacity and the lowest capacity experienced after the event.
- E (Extent): This metric quantifies the *extent* of the disturbance by measuring the duration of the unfavorable state in hours.
- P (Promptness): This metric evaluates how *promptly* the system recovers its resilience levels, i.e., the capacity recovery rate over time.

Each metric is calculated using the resilience curve illustrated in Fig. 1. L corresponds to the difference between the initial health state and the lowest health state experienced by the studied variable during the disturbance process. Thus, the Eq. (3) is used to calculate the metric L:

$$L = SH_0 - SH_{pd} \tag{3}$$

The metric E is calculated as the time during which the system remains in the post-disturbance degraded state, according to Eq. (4):

$$E = t_{er} - t_{ee}. \tag{4}$$

Finally, the metric P is obtained by calculating the dependency of the restorative state according to the Eq. (5):

$$P = \frac{SH_0 - SH_{er}}{T - t_{er}} \tag{5}$$

These metrics provide a quantitative basis for assessing the resilience of electrical systems to seismic events, offering insights into the depth, duration, and speed of recovery following disruptions.

2.2.5. Earthquake resilience assessment

The methodology for assessing the resilience of power systems to seismic events involves a structured multi-step process, detailed as follows:

1. Initialization of Seismic Variables: Randomly selects seismic event characteristics, including the epicenter, intensity, and time of occurrence.
2. PGA Determination: Calculates the PGA at the specific locations of all power plants and system nodes, characterizing the earthquake's impact on the electrical system.
3. Damage Assessment Based on Fragility Curves: Applies the fragility curves of generation units and electrical substations to probabilistically determine the extent of damage to each generator and node. A damaged node is assumed to proportionally reduce the capacity of all connected components, thereby impacting transmission lines and demand.
4. Restoration Curve Analysis: Estimates the time required for system components to fully recover their operational capacity using restoration curves.
5. Formulation of Disconnection and Reconnection Profiles: Develops specific profiles outlining the disconnection and subsequent reconnection processes for each generation technology, transmission line, and nodal demand.
6. Resilience Analysis through REMix: The generated profiles are used as inputs to the REMix framework to analyze the system's resilience under the conditions of the seismic event.

2.3. Case study

This case study evaluates the performance of three hydrogen demand configurations in New Zealand for the year 2050 under earthquake scenarios. The configurations—concentrated, intermediate, and distributed demand—are detailed in Section 2.3.5.

2.3.1. REMix for New Zealand

New Zealand's electricity system has a total capacity of 9.4 GW, of which 7.4 GW (78 %) is renewable. This capacity is distributed across hydroelectric (5.4 GW), fossil fuels (2.2 GW), wind (1.3 GW), and geothermal (1.2 GW) sources [63]. As of 2023, electricity demand was allocated among various sectors: industrial (35 %), residential (33 %), commercial (24 %), agricultural (6 %), and transportation (0.5 %). In 2022, the country generated 39.6 TWh of electricity, with the North Island contributing 22.3 TWh and the South Island contributing 18.4 TWh. Natural gas accounted for 60.51 % of total energy demand, largely driven by industrial use [64].

The 2019 Zero Carbon Act established ambitious goals for achieving net-zero greenhouse gas emissions by 2050 and reducing biogenic methane emissions by 24–47 % relative to 2017 levels [65,66]. This legislation underpins New Zealand's climate change policies, including the Gas and Hydrogen Transition Plan and the Energy Strategy [67]. The hydrogen strategy envisions the production of 560,000 tonnes of green hydrogen annually by 2050, alongside expanding renewable electricity

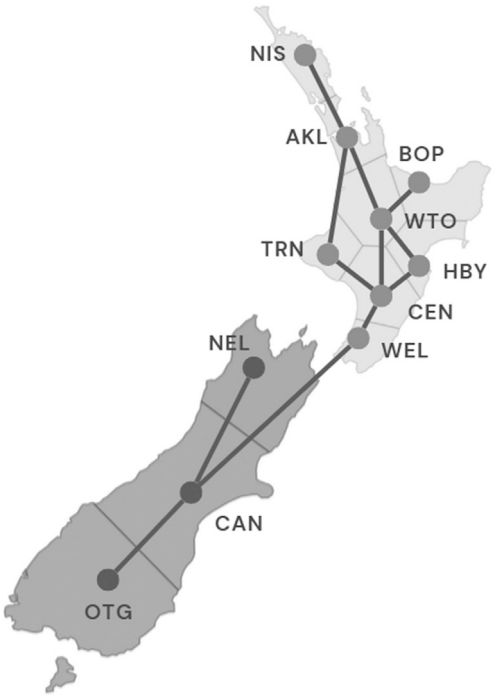

Fig. 5. New Zealand REMix-NZ representative scheme [68].

capacity by 12.5 GW, enabling demand response of 3.8–8.2 TWh, and displacing 1.56–2.26 trillion liters of liquid fuel. These initiatives aim to bolster the country's energy resilience and security.

REMix-NZ [68], based on the open-source REMix framework, is an integrated multi-energy system model tailored for New Zealand. It enables linear deterministic optimization with hourly resolution, capturing the dynamics of the New Zealand electricity system. The model is organized into 11 geographical regions and incorporates nearly 10 generation technologies. Fig. 5 illustrates the regional organization of New Zealand within REMix-NZ.

2.3.2. REMix-NZ: system expansion for 2050

In this study, REMix-NZ is applied exclusively to the electricity sector. The least-cost system configuration for 2050 is determined based on the annual regional demand outlined in Table A.4 and the installed generation capacity in 2024, presented in Table A.5. The available technologies for system expansion (Table A.6) include photovoltaic (PV) systems—central fixed, central tracking azimuth, and decentralized—wind turbines (onshore, offshore floating, and offshore foundation), geothermal plants, hydroelectric facilities, and gas technologies (gas turbine, combined cycle gas turbine, and open cycle gas turbine). Additionally, thermal technologies (biomass, diesel, and coal), battery storage systems, and electrolyzers are considered.

The associated costs and emissions are summarized in Table A.7.

2.3.3. Energy not served

In the model, the cost of electricity not served, referred to as "Slack Cost", is set at 3 million euros per gigawatt-hour (GWh), while the cost of hydrogen demand not served, "H2 Slack Cost", is set at 1.5 million euros per GWh.

In this context, unserved electricity demand excludes the electricity required for hydrogen production. The model treats this separately as hydrogen demand, which is directly tied to the operation of electrolyzers. This differentiation allows the model to capture two distinct aspects of supply constraints: (1) the unserved electricity demand for end-users—households, industries, and commercial sectors (*non-hydrogen not served*)—and (2) the unserved hydrogen demand stemming from the inability to supply electrolyzers (*hydrogen not served*). By assigning a lower Slack Cost to hydrogen, the model prioritizes electricity supply to ensure that critical end-user demand is met before addressing hydrogen production.

The cost differential reflects two considerations. First, hydrogen demand is modeled as a flexible, interruptible load: during scarcity, curtailing electrolyzers is a lower-cost way to relieve the system than shedding end-use electricity. Second, the higher penalty on unserved end-use electricity approximates its larger societal and economic damages, which aligns with the perspective that green hydrogen can serve as a "strategic reserve" to temporarily free capacity for essential services and thereby provide operational flexibility to power systems.

This interpretation is consistent with the concept of the Value of Lost Load (VoLL), commonly understood as society's willingness to pay to avoid an outage. By implicitly valuing unserved end-use electricity more highly than deferred hydrogen production, the model captures the broader social cost of power interruptions while recognizing hydrogen's role in enhancing system flexibility and stability [41].

This prioritization leads the model to favor sacrificing hydrogen production when supply constraints arise, representing the less costly alternative. However, it is important to recognize that if the consequences of unserved demand were more severe—due to extended disruptions or higher societal impacts—both electricity and hydrogen supplies could be simultaneously affected. Highlighting this differentiation and prioritization is crucial for understanding the model's decision-making process across different scenarios and its implications for energy system resilience.

2.3.4. Earthquakes in New Zealand

The parameters for the simulated extreme event correspond to an earthquake with a magnitude of 7.8 on the Richter scale and a depth of 5 km. These values were chosen to represent a high-impact, shallow event consistent with major earthquakes observed in the region, where shallow sources are typically associated with stronger ground shaking and greater damage potential.

The epicenters of the simulated earthquakes are uniformly sampled across the model's 11 regions representing New Zealand. This ensures coverage of events near any electrical node in the system, providing a comprehensive assessment of potential impacts across all model regions. Table B.8 lists the selected epicenters and their geographic distribution, ensuring a wide range of scenarios is evaluated.

The timing of the earthquake is determined by first optimizing the operation of the New Zealand electricity system under normal conditions and identifying the period with the highest marginal costs. The earthquake is set to occur during the 4900th hour of the optimized year, corresponding to a day in June at approximately 1 p.m. Choosing this peak-cost hour intentionally stresses the system, providing a conservative upper-bound estimate of potential disruption and a stringent test of resilience.

The parameters used for the Fragility Functions of generation units and high-voltage substations are provided in Table B.9, while the Restoration Functions for electric power system components are presented in Table B.10.

2.3.5. Hydrogen demand scenarios

The hydrogen demand scenarios for 2050 are derived from projections [42] that quantify hydrogen use for ammonia (fertilizer) and methanol production. The corresponding baseline demands are reported in the first section of Table C.11.

Two additional scenarios are constructed to contrast hydrogen demand spatial configurations: intermediate and concentrated. The

intermediate scenario allocates demand across major centers in New Zealand—Auckland (AKL), Taranaki (TRN), Wellington (WEL), Canterbury (CAN), and Otago (OTG)—as shown in the middle section of Table C.11. In contrast, the concentrated scenario locates all demand in the Taranaki (TRN) region, New Zealand's principal port (last section of Table C.11). The distributed scenario (first section) spreads demand across all model regions and serves as the benchmark in subsequent analyses.

These demand projections follow the Clean Hydrogen Ladder developed for New Zealand by [42], which identifies fertilizer and methanol as the most relevant large-scale applications by 2050. Other potential uses, such as transportation, heating, or long-duration grid balancing, appear further down the ladder and are expected to emerge later. Focusing on fertilizer and methanol, therefore, provides a consistent and robust baseline for modeling, while future diversification of demand centers would further strengthen the resilience benefits of distributed hydrogen layouts.

2.3.6. Simulation parameters

This study analyzes 1,500 simulations corresponding to 500 earthquake events for each of the three hydrogen demand scenarios in New Zealand for 2050: distributed, intermediate, and concentrated. For each scenario, 500 earthquakes are generated uniformly across all model regions, ensuring a comprehensive distribution of epicenters. Each event is simulated over a 300-hour period, with optimization commencing five hours prior to the earthquake's occurrence.

3. Results and analysis

This section analyzes New Zealand's resilience in 2050 with respect to hydrogen production, following the integration of the resilience framework into REMix-NZ. Section 3.1 discusses the results of incorporating shutdown profiles related to natural disasters into REMix-NZ. Section 3.2 examines New Zealand's earthquake vulnerability, and Section 3.3 provides a comparative analysis of earthquake responses across the three hydrogen demand configurations.

The results of the New Zealand electric system expansion for 2050 for each hydrogen demand scenario, obtained from the *Solve Run*, are presented in Appendix D, Table A.7 and Fig. D.13.

3.1. Connection of resilience framework to REMix-NZ

Fig. 6 illustrates the successful integration of the resilience framework into REMix-NZ, using the *Distributed Hydrogen Demand* scenario as a representative case. Fig. 6a compares the results from two distinct optimization runs. The *Solve Run* reflects the initial system expansion and operational behavior projected for 2050 under normal conditions. In contrast, the average electrical generation from 500 *Resilience Runs* demonstrates the system's response to an earthquake-induced HILP event, revealing deviations from normal operation, as shown in Fig. 6b.

The average results from the resilience simulations show that system operations begin to differ from normal, non-contingency operations approximately five-time steps after the optimization begins, coinciding with the timing of earthquake events. Following this, the system experiences significant discrepancies for roughly 100 hours before gradually stabilizing. The pronounced spike observed near the end of this period indicates marked deviations between normal system operation and the average of the resilience runs. This change can be attributed to initial conditions such as reduced availability of renewable resources, particularly solar, and congestion in the HVDC link connecting the North and South Islands.

The analysis of Fig. 6b suggests that it represents the average level of reorganization required by the system in response to an earthquake. This indicator highlights that greater levels of reorganization correspond to increased resource deployment for contingency responses, which were not accounted for under regular operating conditions. These findings demonstrate that integrating the resilience framework with REMix-NZ effectively identifies the occurrence of disruptive events and optimizes system operations under generation and load disconnected profiles.

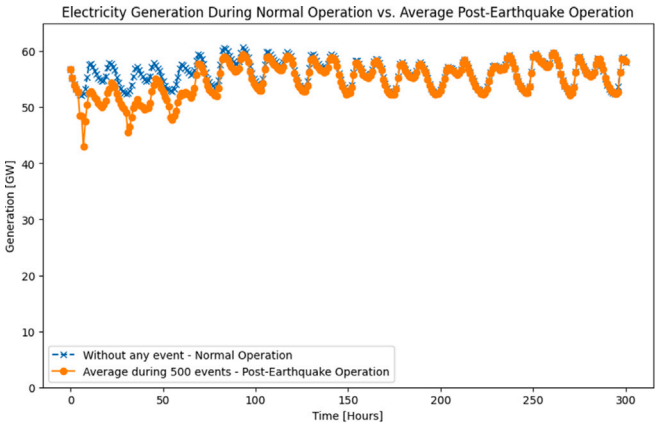

(a) Comparison of electricity generation over time between the normal operation (*Solve Run*) and the average generation during 500 post-earthquake events (*Resilience Run*).

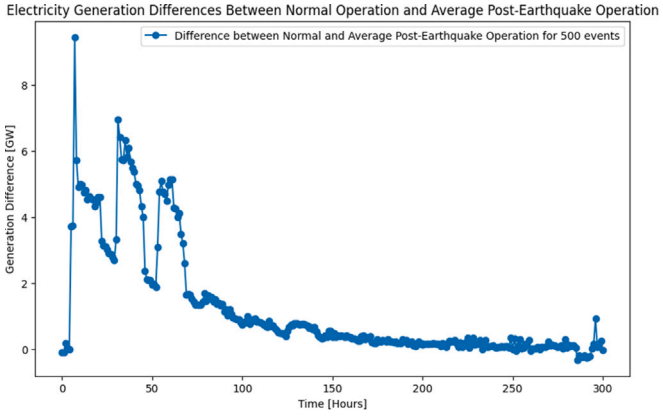

(b) Difference in electricity generation over time between the normal operation (*Solve Run*) and the average of 500 post-earthquake events (*Resilience Runs*).

Fig. 6. Connection verification for REMix-NZ and the resilience framework using the "Distributed Hydrogen Demand" scenario.

Integrating the resilience framework into REMix-NZ facilitates the analysis of system behavior under both normal conditions and earthquake-induced disruptions. Normal operation serves as the baseline for the system's performance in 2050, while the average post-earthquake operation across 500 optimized events highlights deviations caused by seismic events. This integration effectively quantifies the system's reorganization capabilities during contingencies, demonstrating its utility in optimizing operations under disrupted conditions.

3.2. Power system vulnerabilities to earthquakes in New Zealand

New Zealand's position at the Pacific and Australian tectonic plate boundary exposes the country to frequent and unpredictable seismic activity. This inherent risk underscores the importance of assessing the impact of HILP events on the national electrical system to ensure the development of a resilient and robust infrastructure capable of enduring such disruptions.

Fig. 7 depicts the technological distribution of capacity losses resulting from 500 simulated earthquake events in the base scenario with distributed hydrogen demand.

The occurrence of an earthquake affects all technologies, with the most significant impacts concentrated in capacities below 5 MW, as shown at the top of each technology box. However, isolated events can result in disconnections of up to 70 GW, particularly for PV systems

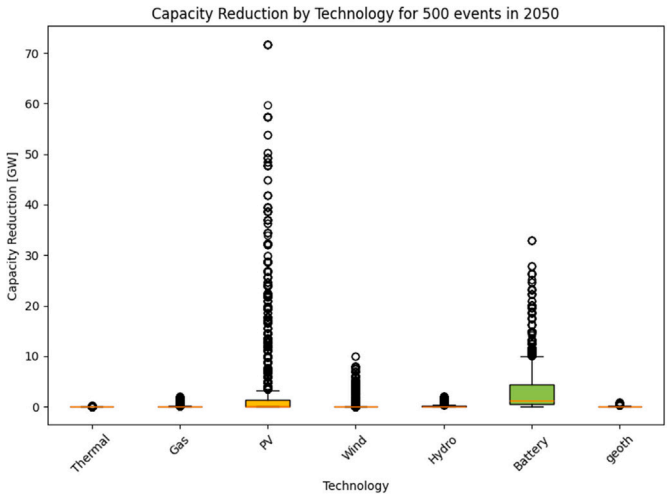

Fig. 7. Box plot of the generation capacity reduction per technology resulting from 500 earthquakes in the 'Distributed Hydrogen Demand' scenario.

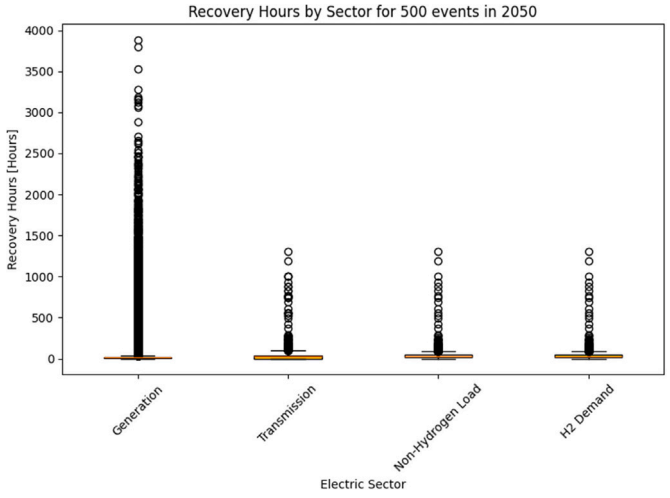

Fig. 8. Box plot of the hours of recovery of 100 % of the operating capacity of each electrical sector resulting from 500 earthquakes in the 'Distributed Hydrogen Demand' scenario.

and batteries, which represent the largest installed capacities in the system. This can be explained by the fragility curves and the high PGA values, which increase the likelihood of severe damage. Additionally, the most extreme cases can be attributed to the nodal representation of the New Zealand system in REMix-NZ, where all regional generation for a specific technology is connected to the grid at a single point. This point coincides with the epicenters selected for the simulated earthquakes.

Fig. 8 illustrates the recovery processes for various system sectors, modeled through the recovery curves of generation units and high-voltage electrical substations.

The restoration of the electricity sector is concentrated within the first 125 hours after an earthquake, with 75 % of the recovery occurring during this time. Notably, restoring transmission capacity enables the reconnection of lost demand, including both hydrogen and non-hydrogen loads, during HILP events. However, recovery within the generation sector spans a longer timeframe, with some units requiring up to 3,500 hours to fully resume operations. This is determined by the standard deviation of the normal distribution representing recovery times for complete damage states, as detailed in Restoration Curves presented in Fig. 4b. It is estimated that 99.9 % of the restoration process is completed within three standard deviations.

The damage to non-hydrogen demand is proportional to the percentage of damage at its connection node, following a similar principle to that of the transmission system. However, as shown in Fig. 8, the impact on the transmission system is more pronounced, as a single node can connect to multiple transmission lines. As a result, when an earthquake damages a node, the capacity of all connected transmission facilities, as well as the associated hydrogen and non-hydrogen demand, is simultaneously reduced.

This study has two main limitations. First, the estimation of damage states and restoration trajectories relies on fragility and recovery curves from the U.S. HAZUS Handbook. While widely applied and technically robust, these curves do not capture New Zealand-specific features such as design standards, construction practices, or maintenance policies. As a result, local assets may perform differently under seismic stress. Nevertheless, applying the same framework consistently across all scenarios preserves the validity of the relative comparison between centralized and distributed hydrogen layouts.

Second, the analysis considers a single earthquake magnitude and depth (7.8 and 5 km), representing the strongest event historically recorded in New Zealand. While this provides a conservative upper bound, variations in magnitude and depth would directly affect PGA values, component damage, and recovery times. In addition, the geographic location of the epicenter is critical: earthquakes in high-hazard regions with softer soils are expected to cause stronger shaking and greater infrastructure damage. A centralized hydrogen hub in such regions would face higher risks than a distributed configuration spread across multiple areas. By focusing on the most extreme documented event, the results provide a cautious but informative benchmark of potential system impacts and recovery trajectories under HILP conditions.

The planning and expansion of New Zealand's electricity system for 2050 indicate that HILP events, such as earthquakes, will inevitably cause damage to system components. Overall, the analysis highlights that damage to system components during HILP events such as earthquakes is unavoidable, underscoring the importance of preventive planning and resilient system design.

3.3. Distributed hydrogen improves resiliency

The integration of hydrogen as both a supply and demand resource necessitates significant system expansion. Meeting this new demand requires strategically utilizing available resources, particularly through increased solar generation and storage capacity, as projected for 2050.

In this context, the critical question is not whether hydrogen will be integrated by 2050 but how the network should be strategically distributed to effectively respond to inevitable events such as earthquakes. This analysis underscores the importance of preventive planning measures aimed at minimizing infrastructure damage and reducing energy deficits caused by disruptions to critical system components.

3.3.1. Resilience metrics

Tables 1 and 2 present the mean and *conditional value at risk* (CVaR at 5 % worst cases) resilience metrics for generation availability and non-hydrogen load, respectively. The metrics for non-hydrogen load include the average and CVaR of the unserved load.

Fig. 9 and Fig. 10 illustrate the average and CVaR *FLEP metric* for the three hydrogen demand scenarios, respectively, based on an average of 500 earthquake events. These metrics facilitate the evaluation of resilience concerning operational aspects, specifically regarding generation availability and the disconnection of non-hydrogen load during such events.

Regarding the average LEP metrics for generation, as shown in Table 1 and Fig. 9, it is evident that, regardless of the hydrogen demand scenario, the deterioration in generation operations is more pronounced than that of non-hydrogen demand. This can be explained by the fact

Table 1
Resilience metrics calculated for the Generation Curve in each hydrogen demand scenario.

Generation Availability						
Resilience Metric	Concentrated		Intermediate		Distributed	
	Mean	CVaR	Mean	CVaR	Mean	CVaR
F	–	–	–	–	–	–
L [%]	26	64	19	44	18	42
E [hrs]	41	285	60	287	39	271
P [GW restored/h]	0,026	0,063	0,019	0,066	0,023	0,211

Table 2
Resilience metrics calculated for the non-hydrogen load curve in each hydrogen demand scenario.

Non-Hydrogen Load Connected						
Resilience Metric	Concentrated		Intermediate		Distributed	
	Mean	CVaR	Mean	CVaR	Mean	CVaR
F	–	–	–	–	–	–
L [%]	6	20	6	19	6	18
E [hrs]	33	197	39	218	35	175
P [GW restored/h]	0,042	0,042	0,045	0,053	0,044	0,034
Not Served [GWh]	47,720	50,240	51,320	54,020	47,700	50,220

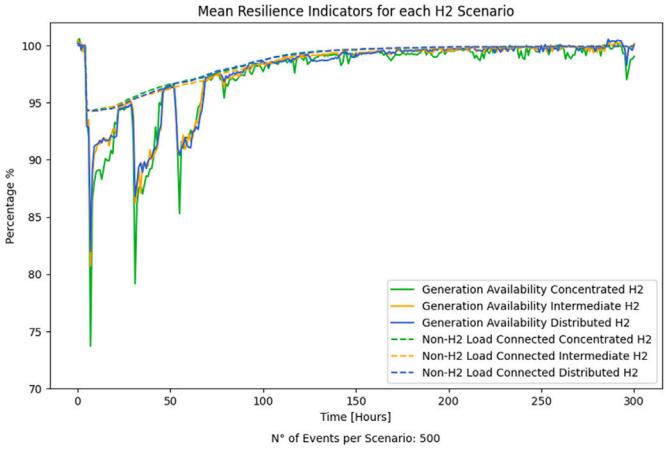

Fig. 9. Mean resilience indicators for generation availability and non-hydrogen load connected across 500 seismic events, comparing concentrated, intermediate, and distributed hydrogen scenarios.

that the loss of non-hydrogen load is exclusively caused by damage at the connection point—specifically, the transmission node. Damage to the transmission node reduces the capacity of all connected elements, including generation facilities. The generation sector experiences more severe impacts, often referred to as "double damage," due to two primary factors: first, fragility curves and PGA values determine the damage to generation facilities; second, damage at the connection point between the grid and generation facilities further exacerbates the situation.

The average resilience metrics indicate that the distributed hydrogen demand scenario is the most resilient, while the concentrated scenario exhibits the lowest resilience due to a more significant initial drop and slower recovery. Conversely, resilience metrics for the 5 % most adverse scenarios reveal that distributed hydrogen demand performs better, with a less pronounced initial drop, faster recovery, and shorter duration of the damage phase. However, it is important to note that in the most extreme cases, full recovery is not achieved within the 300-hour optimization period.

The average resilience of non-hydrogen load to earthquakes demonstrates a similar pattern across all hydrogen demand scenarios. This

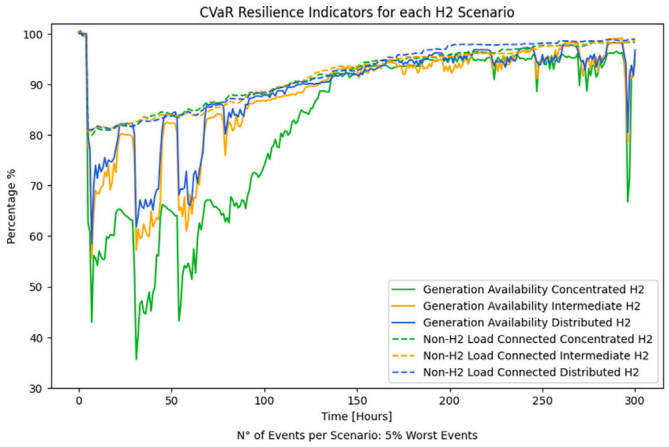

Fig. 10. CVaR resilience indicators for generation availability and non-hydrogen load connected across the 5 % worst seismic events, comparing concentrated, intermediate, and distributed hydrogen scenarios.

behavior is attributed to the damage and subsequent node reconnection to which the demand is linked. These dynamics are outputs of the resilience framework that are incorporated as inputs into REMix-NZ.

An analysis of the 5 % of the most unfavorable cases reveals that the decentralized hydrogen demand scenario slightly improves load resilience.

A closer inspection of each resilience metric, particularly metric L, as shown in Fig. 10, indicates that the concentrated demand scenario experiences the highest average and CVaR degradation for both generation and non-hydrogen load. The location of the earthquake epicenters primarily influences this outcome. In the concentrated demand scenario, earthquakes with epicenters in the North Island—where hydrogen demand and the generation facilities, particularly solar installations, are concentrated—result in more severe impacts. This concentration of infrastructure heightens the risk of disconnection, leading to a more pronounced initial drop in system performance.

Metric E, which measures the extent of system degradation following an earthquake, shows that the distributed hydrogen demand scenario performs best from a generation perspective. In contrast, the intermediate hydrogen scenario represents the worst case. This result can be explained by the differing impacts of damage in the generation sector across scenarios. Since the expansion of each scenario was tailored to its specific characteristics, scenarios with higher demand concentration prompted a corresponding expansion of generation capacity near hydrogen consumption centers. Consequently, these larger clusters of capacity remain disconnected for longer periods, and their reconnection process is slower due to the larger "blocks" involved.

Finally, regarding the speed of system recovery, represented by metric P, the intermediate scenario exhibits the lowest variation per unit of time, indicating the slowest average recovery. This metric is calculated from a recovery level of 96 % of the connected generation capacity to full recovery (100 %), which eliminates the disadvantage previously observed in the intermediate scenario regarding the extent of the damage state. Instead, it highlights that the generation blocks—corresponding to nodal generation by reconnected technology—recover more quickly in this phase, demonstrating a beneficial aspect of this configuration.

In the case of a power supply disruption, generation reconnection occurs more rapidly in the distributed demand scenario. This is due to the slight distribution of generation across nodes, which facilitates faster reconnection, even though no scenario achieves 100 % recovery of the generation capacity.

As evidenced by the results for both generation availability and non-hydrogen load, the 300-hour simulation horizon is effective in capturing the short-term dynamics of disruption and recovery following

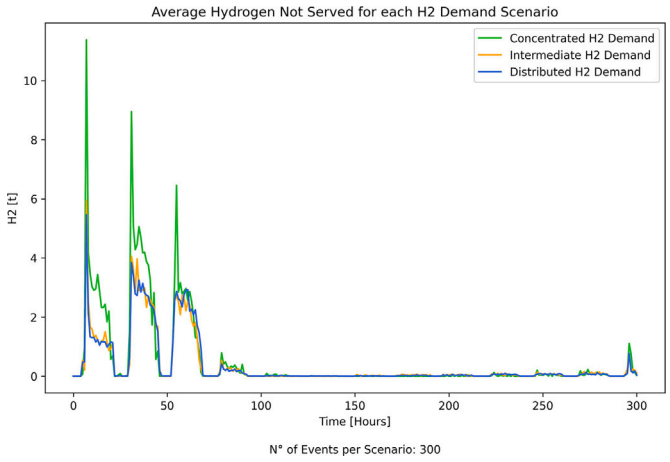

Fig. 11. Comparison of the average Hydrogen Not Served of 500 Resilience Runs over time.

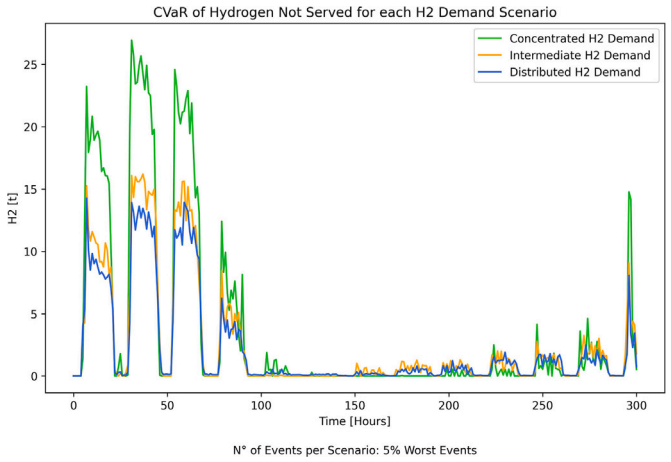

Fig. 12. Comparison of the CVaR Hydrogen Not Served over time of 500 Resilience Runs.

earthquakes. However, this timeframe does not reflect the full duration of infrastructure restoration. Based on the HAZUS recovery functions, units with moderate damage typically return to full operation within the simulated period, whereas those with extensive or complete damage recover only about 60 % of their capacity by 300 hours. Full restoration of severely affected assets is expected to require up to 100 days. These findings indicate that our analysis provides a robust characterization of short-term resilience but does not encompass the complete recovery trajectory. Future research should therefore extend the analysis to include simplified long-term recovery dynamics, complementing the short-term operational perspective developed here.

3.3.2. Energy not served performance

Table 2 presents the non-hydrogen load not served for each hydrogen demand scenario. This metric corresponds to the purchased and sold electricity, excluding the demand associated with electrolyzer operations.

As indicated by the previously analyzed resilience metrics, the plots of non-hydrogen load not served reveal that no scenario consistently exhibits superior or inferior system performance. This is primarily because unserved load is exclusively caused by node damage within the system and insufficient transmission capacity to meet demand. Notably, the model prioritizes electricity supply over hydrogen, as the cost of hydrogen not served is lower than that of electricity not served. This preference accounts for the differences observed between unserved hydrogen and electricity demands. In cases of more severe system impacts, both electricity and hydrogen would likely experience not served demand.

The comparison of hydrogen demand not served for each study scenario is shown in Fig. 11, which presents the average hydrogen not served over time. Additionally, Fig. 12 illustrates the behavior of the worst 5 % of cases.

A detailed analysis of the hydrogen demand not served reveals that the concentrated scenario experiences the highest “sacrifice” of hydrogen supply. This is primarily because this scenario is subjected to the most detrimental conditions for hydrogen supply: earthquakes occurring on the North Island, where the concentrated hydrogen demand is located. Given the system’s flexibility and the relatively low slack cost for hydrogen, the optimal response to such events is to prioritize electricity supply—due to its higher penalty—by sacrificing hydrogen demand. This outcome also indicates that the concentrated system configuration has fewer degrees of freedom to adapt and respond effectively after a contingency.

In addition to the significant disruption caused by earthquakes on the North Island, the concentrated scenario is also heavily affected by seismic events on the South Island. In these cases, the system must continue to supply a highly concentrated demand in the north despite reduced resource availability and increased stress on the interconnection between islands. In the most extreme scenarios, this concentrated hydrogen demand cannot be met, as illustrated by the CVaR metric in Fig. 12.

Table 3
Indicators and resilience metrics for hydrogen load in each hydrogen demand scenario.

Hydrogen Load						
Indicator	Concentrated H2		Intermediate H2		Distributed H2	
N° events w/H2 Not Served	370		436		420	
Resilience Metric	Mean	CVaR	Mean	CVaR	Mean	CVaR
Not Served [t]	115,17	121,23	94,95	99,95	91,85	96,68

3.4. Hydrogen demand performance

To provide a more detailed analysis of hydrogen demand, Table 3 compares the amount of unserved hydrogen across scenarios over the 300-hour recovery horizon.

The results indicate that not all optimized events result in unserved hydrogen demand. This outcome is influenced by the earthquake’s epicenter and the hydrogen demand distribution, which determines whether hydrogen demand should be “sacrificed” to prioritize electricity supply over electrolyzer operation. Table 3 shows that the concentrated scenario has the lowest frequency of unserved events. However, these events carry greater impacts due to the high demand concentration in a single region, which may not coincide with the earthquake’s epicenter, and complicates the ability to fully meet demand.

Fig. D.14 illustrates the average hydrogen production for each demand scenario over the recovery horizon. Immediately after the earthquake, production is consistently lower in the concentrated scenario, highlighting the higher vulnerability of centralized electrolyzers to local failures. In contrast, distributed and intermediate scenarios recover more quickly, and after the initial disruptions, all three trajectories converge with only minor differences. This indicates that the main resilience benefit of distributed layouts is concentrated in the early response phase, rather than in long-term steady production levels.

The analysis of the hydrogen demand not served reveals that it is less frequent in the distributed scenario than in the intermediate scenario and occurs in fewer events. This is notable because distributed hydrogen provides greater operational flexibility during contingencies, reducing the need to curtail electrolyzers. This supports the conclusion that the distributed scenario offers superior infrastructure and load resilience.

Table 3 presents the frequency of hydrogen demand not served for each scenario, including the mean, median, and CVaR at the 5 % level. The CVaR represents an arithmetic measure of expected losses in the worst 5 % of scenarios. A lower CVaR indicates a shorter tail of extreme losses, suggesting that the respective scenario is less likely to experience significant disruptions.

Based on the CVaR metrics presented in Table 3, the results indicate that the "safest" scenario corresponds to distributed hydrogen demand. This is evidenced by the relatively small deviations in average hydrogen demand not served. In contrast, the concentrated scenario shows a clustering of events with low levels of unserved hydrogen but also the most severe outcomes in extreme cases. The intermediate scenario does not display a consistent pattern of superior or inferior performance, supporting the conclusion that these configurations are less favorable for electricity system expansion on average.

The analysis shows that distributed hydrogen demand materially enhances system resilience relative to concentrated and intermediate layouts. It lowers both the frequency and severity of unmet hydrogen and non-hydrogen load during earthquakes and shortens recovery times. Concentrated demand experiences the largest disruptions—owing to the exposure of centralized assets, especially under North Island earthquakes—whereas the intermediate layout tends to recover more slowly and inconsistently.

Under normal operating conditions, the distributed scenario is also more cost-effective (Table D.12), with lower investment and operating needs driven by reduced fossil reliance and less transmission stress. In contrast, concentrated demand forces large energy transfers into a single node, increasing costs and operational risks.

The theoretical rationale mirrors evidence from distributed energy resources and microgrids [69]: spreading supply across nodes removes single points of failure, adds redundancy, and supports local restoration. Regionally distributed hydrogen hubs therefore, act as resilience buffers that maintain supply despite localized outages.

Overall, distributed hydrogen demand emerges as the most robust and economical configuration, minimizing disruptions and enhancing system adaptability to HILP events.

4. Conclusions and future work

This study developed a resilience framework for energy systems planning with hydrogen. By modeling stochastic damages resulting from unexpected, high-impact hazards and connecting the derived disconnection profiles to a capacity-expansion optimization model, we quantified which hydrogen architecture—distributed, intermediate, or concentrated—offered the most robust response. This framework is methodologically applicable to any country, provided that local hazard parameters, fragility data, and recovery functions are adapted to the local context; in this study, we quantified the resilience of these hydrogen architectures against seismic events in New Zealand's energy transition.

The simulations demonstrate the successful integration of the resilience framework into the REMix-NZ energy system optimization tool. These simulations revealed clear differences between normal system operations and those under post-earthquake conditions. The findings underscore the importance of flexibility and adaptability in mitigating the impacts of high-impact, low-probability (HILP) events, highlighting the framework's potential to inform resilient energy planning in New Zealand and elsewhere.

The distributed hydrogen demand scenario consistently exhibited superior resilience, minimizing disruptions to both electricity and hydrogen demand. This performance highlights the critical role of flexibility in mitigating seismic impacts and the importance of decentralized infrastructure. Metrics such as non-hydrogen load, unmet hydrogen demand, and the system's state of health—measuring speed, depth, extent, and recovery promptness—further underscore this finding. In contrast, the concentrated scenario demonstrated the greatest vulnerability, with significant disruptions observed across various epicenters. Beyond resilience, the distributed scenario also proved more cost-effective, combining lower investment and operating costs with reduced dependence on fossil fuels. Taken together, these benefits position distributed hydrogen demand as the most robust and economically efficient option for future energy systems.

Future research should also address several model limitations identified in this study. First, considering a wider range of earthquake magnitudes and depths would allow for a more comprehensive characterization of seismic impacts. Second, extending the simulation horizon beyond 300 hours is necessary to capture long-term recovery dynamics that may span months. Third, varying the timing of earthquake occurrences across different operating conditions could provide further insights into system performance under alternative stress scenarios. Finally, explicitly analyzing the influence of different epicenter locations and site conditions would highlight how regional hazard variability shapes resilience outcomes. Addressing these aspects will strengthen the framework and provide further evidence for the earthquake resilience and cost-effectiveness of distributed hydrogen layouts.

While this study focused on seismic events in New Zealand, the proposed resilience framework is versatile and can be applied to other regions and natural disasters worldwide. It offers engineers and system planners a practical tool to guide infrastructure siting and investment choices, supporting the assessment of trade-offs between centralized and distributed configurations. Expanding the methodology to include additional high-impact, low-probability events—such as hurricanes, floods, and wildfires—as well as extending it to the heat and transport sectors, would provide a more holistic perspective on resilient energy planning. This versatility is facilitated by REMix's flexibility as an open-source capacity-expansion platform.

CRediT authorship contribution statement

Melissa Alé: Writing – review & editing, Writing – original draft, Visualization, Validation, Methodology, Investigation, Formal analysis, Data curation, Conceptualization. **Madhura Yeligeti:** Writing – review & editing, Validation, Software, Resources, Methodology, Conceptualization. **Rafaella Canessa:** Writing – review & editing, Validation, Resources, Conceptualization. **Manuel Wetzel:** Writing – review & editing, Validation, Software, Resources, Conceptualization. **Rodrigo Moreno:** Writing – review & editing, Validation, Supervision, Methodology, Conceptualization. **Rebecca Peer:** Writing – review & editing, Validation, Supervision, Project administration, Funding acquisition. **Hans-Christian Gils:** Writing – review & editing, Validation, Supervision, Project administration, Funding acquisition. **Jannik Haas:** Writing – review & editing, Validation, Supervision, Project administration, Methodology, Funding acquisition, Conceptualization.

Declaration of generative AI and AI-assisted technologies in the writing process

During the preparation of this work, the author(s) utilized ChatGPT to assist with language flow. After using this tool/service, the author reviewed and edited the content as needed and take full responsibility for the publication's content.

Declaration of competing interest

The authors declare the following financial interests/personal relationships that may be considered as potential competing interests:

Jannik Haas reports financial support was provided by New Zealand Ministry of Business Innovation and Employment. Rebecca Peer reports financial support was provided by New Zealand Ministry of Business Innovation and Employment. Hans-Christian Gils reports financial support was provided by German Federal Ministry for Economic Affairs and Climate Action. If there are other authors, they declare that they have no known competing financial interests or personal relationships that could have appeared to influence the work reported in this paper.

Acknowledgments

We thank the HINT project (New Zealand-German Platform for Green Hydrogen Integration), funded by the Catalyst: Strategic Fund and administered by the Ministry of Business, Innovation and Employment of New Zealand, alongside the German Federal Ministry of Education and Research (grant number 03SF0690). M.Y. and H.C.G. also acknowledge support from the ReMoDigital project, funded by the German Federal Ministry of Economy and Energy (grant number 03IE1020B). Additionally, M.A. and R.M. thank the Ministry of Energy of the Government of Chile for their support.

Appendix A. REMix-NZ input data

Table A.4
Projection of the electricity demand by region for New Zealand in the year 2050.

Model Region	Electricity Demand [TWh/year]
AKL	20
BOP	6.5
CAN	16
CEN	4.9
HBY	4.4
NEL	3.0
NIS	4.8
OTG	21
TRN	2.2
WEL	7.2
WTO	8.5
Global	99

Table A.5
Installed generation capacity of the New Zealand power system in 2024.

Tech	Region											Total [MW]
	AKL	BOP	CAN	CEN	HBY	NEL	NIS	OTG	TRN	WEL	WTO	
Wind	-	-	-	522	-	1	-	111	133	223	64	1,054
Geoth	-	175	-	-	-	-	25	-	-	-	836	1,036
Hydro	-	247	1,717	414	149	76	5	1,793	41	-	1,015	5,457
GT	179	37	-	-	-	-	-	-	439	10	804	1468
CCGT	-	-	-	-	-	-	-	-	-	-	385	385
OCGT	55	10	-	-	155	-	-	-	435	-	92	747
Biomass	16	-	3	-	-	-	10	-	-	4	5	37
Diesel	-	-	-	-	-	3	18	-	-	-	–	21
Coal	112	-	-	-	-	-	-	-	-	-	–	112
Total	361	469	1,721	935	304	81	58	1,904	1,048	237	3,201	10,318

Table A.6
Potential installable capacity for each technology per model region for 2050.

Tech	Region											Total [GW]
	AKL	BOP	CAN	CEN	HBY	NEL	NIS	OTG	TRN	WEL	WTO	
PV Central Fixed	181	238	1,084	497	259	477	240	1,165	156	153	387	4,837
PV Central Track Azimuth	181	238	1,074	497	259	476	240	1,153	156	153	387	4,814
PV Decentral	2	1	1	1	0	0	0	0	0	1	1	8
Wind Offshore Floating	35	22	68	6	16	93	47	157	71	15	15	543
Wind Offshore Foundation	13	6	25	2	6	13	5	10	9	1	2	91
Wind Onshore	8	11	32	17	10	15	10	35	7	6	15	166
Total	418	515	2,285	1,019	550	1,074	542	2,520	398	329	806	10,458

Table A.7
Costs and emissions by generation technology.

Tech	CAPEX [€/kWel]	OPEX Fix [€/(kWel a)]	OPEX Var [€/kWel]	Lifetime [years]	CO2 Emissions [€/tCO2]
PV	166	3.70	0	40	0
Wind	900	18	0	25	0
Geothermal	3610	80	0	40	0
Hydro	1650	49.5	0.003	50	0
GT	475	14.25	0.011	35	150
CCGT	775	19.38	0.002	35	150
OCGT	475	14.25	0.011	35	150
Biomass	1830	32.9	0.004	25	150
Diesel	830	27.9	0.004	30	150
Coal	1600	20	0.001	45	150
Battery	61	1.71	0	20	0
Electrolyzer	350	2.59	0	35	0

Appendix B. Earthquake resilience modeling

Table B.8
Set of parameters and earthquake epicenters with uniform distribution for event simulation.

Region	Number of Earthquakes	Magnitude	Depth [km]	epi_x [°]	epi_y [°]
AKL	46	7.8	5	−36,95	174,86
BOP	46	7.8	5	−37,99	176,83
CAN	45	7.8	5	−43,86	171,34
CEN	45	7.8	5	−40,28	175,64
HBY	46	7.8	5	−39,55	176,82
NEL	45	7.8	5	−41,67	172,87
NIS	45	7.8	5	−35,88	174,47
OTG	46	7.8	5	−45,48	169,32
TRN	46	7.8	5	−39,33	174,32
WEL	45	7.8	5	−41,15	174,98
WTO	45	7.8	5	−38,42	175,80

Table B.9
PGA Fragility Functions for generation units and electric substations.

Component	Damage State	Median (g)	β
Small Generation Units (less 100 MW)	Slight	0.1	0.6
	Moderate	0.2	0.6
	Extensive	0.5	0.5
	Complete	0.8	0.5
Large Generation Units (more than 100 MW)	Slight	0.1	0.6
	Moderate	0.3	0.6
	Extensive	0.5	0.6
	Complete	0.9	0.6
High Voltage Substations	Slight	0.1	0.5
	Moderate	0.2	0.5
	Extensive	0.2	0.4
	Complete	0.5	0.4

Table B.10
Restoration Functions for Electric Power System Components.

Component	Damage State	Median (days)	σ (days)
Generation Facilities	Slight	0.5	0.1
	Moderate	3.6	3.6
	Extensive	22	21
	Complete	65	30
Electric Substations	Slight	1	0.5
	Moderate	3	1.5
	Extensive	7	3.5
	Complete	30	15

Appendix C. Hydrogen demand scenarios

Table C.11
Regional demand for hydrogen under each hydrogen demand scenario, based on the projection presented in [42].

Region	Annual Demand [kt]	Hourly Demand [t]
Distributed H2 Demand Scenario		
NIS	1.0	0.1
AKL	71	8
WTO	12	1
BOP	12	1
HBY	13	1
TRN	62	7
CEN	12	1
WEL	35	4
NEL	9.2	1.0
CAN	39.3	4.5
OTG	18.8	2.1
Total	284	36.0
Intermediate H2 Demand Scenario		
AKL	84	9.5
TRN	86	9.8
WEL	48	5.4
CAN	48	5.5
OTG	19	2.1
Total	284	36.0
Concentrated H2 Demand Scenario		
TRN	284	36.0

Appendix D. New Zealand power system expansion for 2050

Table D.12
Details of New Zealand's electricity system costs under each hydrogen demand scenario.

Cost Indicator [MEUR]	H2 Scenario Centralized	Intermediate	Distributed
Fuel Cost	1,198.21	852.59	868.43
Biomass	0.13	0.13	0.11
Gas	1,198.08	852.46	868.32
Coal	0.27	0.29	0.25
Diesel	0.22	0.20	0.17
CAPEX	18,557.45	16,324.34	16,320.18
Battery	5,079.21	4,637.78	4,659.24
Biomass	0.11	0.11	0.10
Gas	3,490.80	2,594.09	2,596.75
Coal	0.17	0.17	0.15
Diesel	0.16	0.17	0.15
Electrolyzer	1,163.39	1,043.85	1,043.80
Geothermal	215.07	215.07	215.07
Transmission Lines	1,521.73	911.58	902.31
Hydro	0.04	0.05	0.04
PV	7,661.88	6,915.59	7,016.53
Wind	2,325.45	2,176.76	2,047.56
OPEX Fix	228.96	137.16	135.76
Transmission Lines	228.96	137.16	135.76
Total [MEUR]	19,984.62	17,314.09	17,324.37

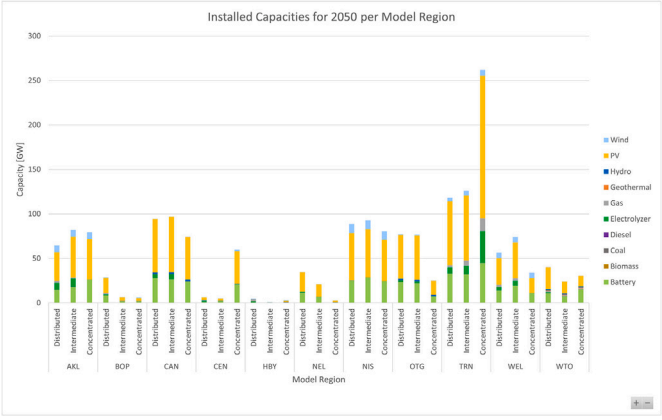

Fig. D.13. Installed capacities by technology in each hydrogen scenario for the year 2050 according to the New Zealand model region.

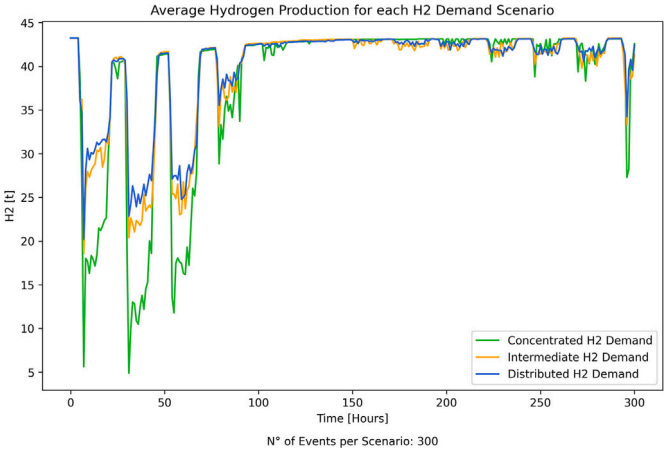

Fig. D.14. Average hydrogen production in each hydrogen scenario for the year 2050.

Data availability

Data will be made available on request.

References

[1] Edenhofer O, Pichs-Madruga R, Sokona Y, Seyboth K, Matschoss P, Kadner S, Zwickel T, Eickemeier P, Hansen G, Schlömer S, von Stechow C. Renewable Energy sources and climate change mitigation. Cambridge, United Kingdom and New York, NY, USA: Cambridge University Press; 2011.

[2] González-Inostroza P, Rahmann C, Alvarez-Malebrán R, Haas J, Nowak W, Rehtanz C. The role of fast frequency response of Energy storage systems and renewables for ensuring frequency stability in future low-inertia Power systems. Sustainability May. 2021;13:5656. https://doi.org/10.3390/su13105656

[3] Panteli M, Moreno R, Martinez C, Alejandro AE, Mancarella P. Flexibility and resilience in future low-carbon Energy systems, In: 17th Int. Conf. on Probabilistic Modelling Applied to Power Systems; 2022 Manchester, United Kingdom.

[4] Strbac G, Kirschen D, Moreno R. Reliability standards for the operation and planning of future electricity networks. Electr Energy Syst Dec. 2016;1(3):143–219. https://doi.org/10.1561/3100000001

[5] Paik S, An SI, Min SK, King AD, Kim SK. Emergent constraints on future extreme precipitation intensification: from global to continental scales. Weather Clim Extremes Dec. 2023;42:100613. https://doi.org/10.1016/j.wace.2023.100613

[6] Haas J, Cebulla F, Cao K, Nowak W, Palma-Behnke R, Rahmann C, Mancarella P. Challenges and trends of energy storage expansion planning for flexibility provision in low-carbon power systems – a review. Renew Sustain Energy Rev Dec. 2017;80:603–19. https://doi.org/10.1016/j.rser.2017.05.201

[7] Moreno R, Panteli M, Mancarella P, Rudnick H, Lagos T, Navarro A, Ordonez F, Araneda J. From reliability to resilience: planning the grid against the extremes. IEEE Power Energy Mag July-Aug 2020;18(4):41–53. https://doi.org/10.1109/MPE.2020.2985439

[8] Haas J, Nowak W, Palma-Behnke R. Multi-objective planning of energy storage technologies for a fully renewable system: implications for the main stakeholders in Chile. Energy Policy Mar. 2019;126:494–506. https://doi.org/10.1016/j.enpol.2018.11.034

[9] Haas J, Cebulla F, Nowak W, Rahmann C, Palma-Behnke R. A multi-service approach for planning the optimal mix of energy storage technologies in a fully-renewable power supply. Energy Convers Manag Dec. 2018;178:355–68. https://doi.org/10.1016/j.enconman.2018.09.087

[10] Khan T, Yu M, Waseem M. Review on recent optimization strategies for hybrid renewable energy system with hydrogen technologies: state of the art, trends and future directions. Int J Hydrogen Energy Jul. 2022;47(60):25155–201. https://doi.org/10.1016/j.ijhydene.2022.05.263

[11] PyPSA. Introduction. [Online.] Available: https://pypsa.readthedocs.io/en/latest/introduction.html [Accessed Apr 12, 2024].

[12] PyPSA. Contingency analysis. [Online.] Available: https://pypsa.readthedocs.io/en/latest/contingency_analysis.html [Accessed Apr 12, 2024].

[13] FINE. ETHOS.FINE - Framework for integrated Energy system assessment. [Online.] Available: https://vsa-fine.readthedocs.io/en/latest/ [Accessed Apr 12, 2024].

[14] Wetzel M, et al., REMix: a GAMS-based framework for optimizing energy system models. J Open Source Softw 2024;9(99):6330. https://doi.org/10.21105/joss.06330

[15] CPLEX. [Online.] Available: https://www.ibm.com/es-es/products/ilog-cplex-optimization-studio [Accessed Aug. 31, 2024].

[16] GUROBI. Gurobi optimization. [Online.] Available: https://www.gurobi.com/ [Accessed Aug 31, 2024].

[17] Gils HC, Scholz Y, Pregger T, de Tena DL, Heide D. Integrated modeling of variable renewable energy-based power supply in Europe. Energy Mar. 2017;123:173–88. https://doi.org/10.1016/j.energy.2017.01.115

[18] Gils HC, Gardian H, Schmugge J. Interaction of hydrogen infrastructures with other sector coupling options towards a zero-emission energy system in Germany. Renewable Energy Dec. 2021;180:140–56. https://doi.org/10.1016/j.renene.2021.08.016

[19] Panteli M, Mancarella P. Influence of extreme weather and climate change on the resilience of power systems: impacts and possible mitigation strategies. Electr Power Syst Res Oct. 2015;127:259–70. https://doi.org/10.1016/j.epsr.2015.06.012

[20] Bruneau M, Chang S, Eguchi R, Lee G, O'Rourke T, Reinhorn A, Shinozuka M, Tierney K, Wallace W, Winterfeldt D. A framework to quantitatively assess and enhance the seismic resilience of communities, In: 13th World Conf. on Earthquake Engineering; Vancouver, B.C., Canada; 2004. p. 19. https://doi.org/10.1193/1.1623497

[21] Ayyub B. Systems resilience for multihazard environments: definition, metrics, and valuation for decision making. Risk Anal 2013;34(2), Feb. 2014. https://doi.org/10.1111/risa.12093

[22] Gasser P, Lustenberger P, Cinelli M, Kim W, Spada M, Matteo B, Peter H, Stefan S, Bozidar S, Tianyin S. A review on resilience assessment of energy systems. Sustain Resil Infrastruct Jun. 2019;6:1–27. https://doi.org/10.1080/23789689.2019.1610600

[23] Panteli M, Trakas DN, Mancarella P, Hatziargyriou ND. Power systems resilience assessment: hardening and smart operational enhancement strategies. Proc IEEE Jul. 2017;105(7):1202–13. https://doi.org/10.1109/JPROC.2017.2691357

[24] Raoufi H, Vahidinasab V, Mehran K. Power systems resilience metrics: a comprehensive review of challenges and outlook. Sustainability Nov. 2020;12(22):9698. https://doi.org/10.3390/su12229698

[25] Bhusal N, Abdelmalak M, Kamruzzaman M, Benidris M. Power system resilience: current practices, challenges, and future directions. IEEE Access 2020;8, Jan. https://doi.org/10.1109/ACCESS.2020.2968586

[26] Schweikert A, Nield L, Otto E, Dienert M. Resilience and critical Power system infrastructure. Colorado, USA: World Bank Group; 2019.

[27] Espinoza S, Panteli M, Mancarella P, Rudnick H. Multi-phase assessment and adaptation of power systems resilience to natural hazards. Electr Power Syst Res Jul. 2016;136:352–61. https://doi.org/10.1016/j.epsr.2016.03.019

[28] Yang Y, Tang W, Liu Y, Xin Y, Wu Q. Quantitative resilience assessment for Power transmission systems under typhoon weather. IEEE Access Jul. 2018;6:40747–56. https://doi.org/10.1109/ACCESS.2018.2858860

[29] Miller R. Resilience assessment of active distribution networks, Ph.D. dissertation, Montana, USA: Norm Asbjornson College of Engineering, Montana State University-Bozeman; 2021.

[30] Hou H, Tang J, Zhang Z, Wang Z, Wei R, Wang L, He H, Wu X. Resilience enhancement of distribution network under typhoon disaster based on two-stage stochastic programming. Applied Energy May. 2023;338:120892. https://doi.org/10.1016/j.apenergy.2023.120892

[31] Lagos T, Moreno R, Navarro A, Panteli M, Sacaan R, Ordonez F, Rudnick H, Mancarella P. Identifying optimal portfolios of resilient network investments against natural hazards, with applications to earthquakes, In: IEEE Transactions on Power Systems; Oct. 2019. https://doi.org/10.1109/TPWRS.2019.2945316

[32] Cheng B, Nozick L, Dobson I. Investment planning for earthquake-resilient electric power systems considering cascading outages. Earthq Spectra Feb. 2022;38(3):1734–60. https://doi.org/10.1177/87552930221076870

[33] Villamarín-Jácome A, Moreno R. Seismic resilience assessment of electric Power systems using a substation Bay-level Model, In: 17th Int. Conf. on Probabilistic Methods Applied to Power Systems Manchester, United Kingdom; 2022. p. 1–6. https://doi.org/10.1109/PMAPS53380.2022.9810625

[34] Sacaan R, Rudnick H, Lagos T, Ordóñez F, Navarro-Espinosa A, Moreno R. Improving power system reliability through optimization via simulation, In: 2017 IEEE Manchester PowerTech; Manchester, UK; 2017. p. 1–6. https://doi.org/10.1109/PTC.2017.7981193

[35] Saltos-Rodríguez M, Aguirre-Velasco M, Velásquez-Lozano A, Villamarín-Jácome A, Haro JR, Ortiz-Villalba D. Resilience assessment in electric Power systems against volcanic eruptions, In: Case on Lahars Occurrence, in 2021 IEEE Green Technologies Conference; Denver, CO, USA; 2021. p. 305–11. https://doi.org/10.1109/GreenTech48523.2021.00056

[36] Liu H, Wang C, Ju P, Li H. A sequentially preventive model enhancing power system resilience against extreme-weather-triggered failures. Renewable Sustain Energy Rev Mar. 2022;156:111945. https://doi.org/10.1016/j.rser.2021.111945

[37] Poudyal A, Lamichhane S, Dubey A, Prado JC. Resilience-driven planning of electric Power systems against extreme weather events. Nov 2023. https://doi.org/10.48550/arXiv.2311.15117

[38] Johnson B, Chalishazar V, Cotilla-Sanchez E, Brekken TK. A Monte Carlo methodology for earthquake impact analysis on the electrical grid. Electr Power Syst Res Jul. 2020;184:106332. https://doi.org/10.1016/j.epsr.2020.106332

[39] Chalishazar V, Huo C, Fox I, Hagan T, Cotilla-Sanchez E, Jouanne AV, Zhang J, Brekken T, Bass. RB. Modeling power system buses using performance based earthquake engineering methods, In: 2017 IEEE Power & Energy Society General Meeting; Chicago, IL, USA. Jul. 2017. p. 1–5. https://doi.org/10.1109/PESGM.2017.8274307

[40] Panteli M, Mancarella P, Trakas DN, Kyriakides E, Hatziargyriou ND. Metrics and quantification of operational and infrastructure resilience in Power systems. IEEE Trans Power Syst Nov. 2017;32(6):4732–42. https://doi.org/10.1109/TPWRS.2017.2664141

[41] Alvear C, Haas J, Palma-Behnke R, Peer R, Medina JP, Kern JD. Green hydrogen exports in New Zealand and Chile can improve electricity supply security if configured as local energy insurance. Energy Sept 2024;304:131930. https://doi.org/10.1016/j.energy.2024.131930

[42] Ghadim HV, Peer RAM, Read EG, Haas J. How much hydrogen could we need in New Zealand? Understanding the diverse hydrogen applications and their regional mapping. J R Soc N Z Mar. 2024:1–20. https://doi.org/10.1080/03036758.2024.2365306

[43] Mucci S, Mitsos A, Bongartz D. Power-to-X processes based on pem water electrolyzers: a review of process integration and flexible operation. Comput Chem Eng Jul. 2023;175:108260. https://doi.org/10.1016/j.compchemeng.2023.108260

[44] Püschel-Løvengreen S, Mhanna S, Apablaza P, Mancarella P, Bukenberger J, Ortega-Vazquez M. Assessing flexibility, risk, and resilience in low-carbon power system planning under deep uncertainty. Melbourne, Australia: University of Melbourne for CSIRO; 2023.

[45] Jordehi AR, Mansouri SA, Tostado-Véliz M, Iqbal A, Marzband M, Jurado F. Industrial energy hubs with electric, thermal and hydrogen demands for resilience enhancement of mobile storage-integrated power systems. Int J Hydrogen Energy Jan. 2024;50:77–91. https://doi.org/10.1016/j.ijhydene.2023.07.205

[46] Cardenas A. An operational resilience objective to integrate in capacity expansion models for green hydrogen production through hres, MSc dissertation, Santiago, CL: Department of Electrical Engineering, University of Chile; 2023.

[47] Haggi H, Sun W, Fenton JM, Brooker P. Proactive scheduling of hydrogen systems for resilience enhancement of distribution networks, In: 2021 IEEE Kansas Power and Energy Conference; Manhattan, KS, USA; 2021. p. 1–5. https://doi.org/10.1109/KPEC51835.2021.9446230

[48] Ministry of Business, Innovation and employment Hıkina Whakatutuki, Interim hydrogen Roadmap. 2024, MBIE, New Zealand.

[49] Handique A, Peer R, Haas J, Osorio-Aravena JC, Reyes-Chamorro L. Distributed hydrogen systems: a literature review. Int J Hydrogen Energy Oct. 2024;85:427–39. https://doi.org/10.1016/j.ijhydene.2024.08.206

[50] Meares T, Tyrell H, Pendlebury R. Hydrogen: the role of the hydrogen production industry in providing system services to the nem. Sydney, Australia: AEMC; 2022.

[51] Sasanpour S, Cao K-K, Gils HC, Jochem P. Strategic policy targets and the contribution of hydrogen in a 100 % renewable European power system. Energy Rep Nov. 2021;7:4595–608. https://doi.org/10.1016/j.egyr.2021.07.005
[52] Plazas-Niño FA, Yeganyan R, Cannone C, Howells M, Borba B, Quirós-Tortós J. Open energy system modeling for low-emission hydrogen roadmap planning: the case of Colombia. Energy Strateg Rev May. 2024;53:101401. https://doi.org/10.1016/j.esr.2024.101401
[53] Constantin A. Nuclear hydrogen projects to support clean energy transition: updates on international initiatives and iaea activities. Int J Hydrogen Energy Feb. 2024;54:768–79. https://doi.org/10.1016/j.ijhydene.2023.09.250
[54] Park C, Koo M, Woo J, Hong BI, Shin J. Economic valuation of green hydrogen charging compared to gray hydrogen charging: the case of South Korea. Int J Hydrogen Energy Apr. 2022;47(32):14393–403. https://doi.org/10.1016/j.ijhydene.2022.02.214
[55] Dong Y, Han Z, Li C, Ma S, Ma Z. Research on the optimal planning method of hydrogen-storage units in wind–hydrogen energy system considering hydrogen energy source. Energy Rep Oct. 2023;9:1258–64. https://doi.org/10.1016/j.egyr.2023.05.116
[56] Modu B, Abdullah MP, Bukar AL, Hamza MF, Adewolu MS. Energy management and capacity planning of photovoltaic-wind-biomass energy system considering hydrogen-battery storage. J Energy Storage Dec. 2023;73:109294. https://doi.org/10.1016/j.est.2023.109294
[57] Li Z, Xia Y, Bo Y, Wei W. Optimal planning for electricity-hydrogen integrated energy system considering multiple timescale operations and representative time-period selection. Applied Energy May. 2024;362:122965. https://doi.org/10.1016/j.apenergy.2024.122965
[58] Dahal S, Karki NR. Transmission systems resilience assessment: a case study in integrated Nepal Power system, In: 10th IOE Graduate Conf; 2021 Pokhara, Nepal.
[59] Yeligeti M, Gils HC, Sasanpour S, Gardian H. Resilience monitoring of future sector-coupled energy systems in, In: STRise 1st International Symposium of Energy System Analysis; Stuttgart, Germany; 2024.
[60] Manjunath M, Gils HC, Yeligeti M, Fyta M, Haas J, Nowak W. Monitoring resilience of future energy systems, MSc Dissertation, Stuttgart, DE: Faculty of Energy, Process Engineering and Biotechnology, University of Stuttgart; 2020.
[61] Crouse CB. Crouse ground-motion attenuation equations for earthquakes on the cascadia subduction zone. Earthq Spectra May. 1991;7(2):201–36.
[62] FEMA. Hazus earthquake Model technical manual, Hazus 4.2 SP3 [Online], Oct 2020. Available https://www.fema.gov/sites/default/files/2020-10/fema_hazus_earthquake_technical_manual_4-2.pdf.
[63] Transpower. Consolidated live data. [Online.] Available: https://www.transpower.co.nz/system-operator/live-system-and-market-data/consolidated-live-data [Accessed Apr 12, 2024].
[64] Ministry of Business. Energy in New Zealand 23. In: Innovation and employment Hıkina Whakatutuki. Wellington, New Zealand: MBIE; 2023.
[65] New Zealand Parliamentary Counsel Office/Te Tari Tohutohu Paremata. Climate change response (zero carbon) amendment act 2019. New Zealand: New Zealand Government; 2019.
[66] Ministry for the Environment Manatu Mo Te Taiao. Climate change response (zero carbon) amendment act 2019. Online. Available: https://environment.govt.nz/acts-and-regulations/acts/climate-change-response-amendment-act-2019/ [Accessed: May 9, 2024].
[67] Ministry of Business. Terms of reference - New Zealand Energy strategy. In: Innovation and employment Hıkina Whakatutuki. New Zealand: MBIE; 2022.
[68] Canessa R, Peer R, Wetzel M, Gils HC, Gulagi A, Breyer C, Osorio-Aravena JC, Haas J. Optimising New Zealand's Energy transition: introducing REMix-NZ's insights into transition pathways and green hydrogen export scenarios. J Clean Prod (Submitted) Jun 2025.
[69] Moreno R, Trakas DN, Jamieson M, Panteli M, Mancarella P, Strbac G, Marnay C, Hatziargyriou N. Microgrids against wildfires: distributed Energy resources enhance system resilience. IEEE Power Energy Mag Jan.–Feb. 2022;20(1):78–89. https://doi.org/10.1109/MPE.2021.3122772